

## DIFFUSION IN THE STANDARD MAP

Itzhack DANA† and Shmuel FISHMAN

*Department of Physics, Technion-Israel Institute of Technology, Haifa 32000, Israel*

Received 21 September 1984

Revised manuscript received 8 January 1985

Diffusion in the standard map is studied numerically. The stochasticity parameter  $K$  is near the critical value  $K_c$ , and the diffusion coefficient  $D$  is calculated. It is found to satisfy to a good approximation the scaling relation  $D \propto (K - K_c)^\eta$ , with  $\eta$  in good agreement with the value predicted by the scaling theory of the disappearance of the last bounding KAM torus. The critical region where this scaling relation holds is surprisingly large, i.e.  $K \leq 2.5$ . The mechanism of transport from the chaotic region to the remnants of the last KAM torus is investigated. Evidence for the existence of a narrow stochastic channel mediating this transport is presented and its origin is discussed. Although the scaling of  $D$  agrees with the predictions of the scaling theory the transport mechanism is different from the one assumed in this theory.

### 1. Introduction

Chaotic motion in Hamiltonian or area-preserving maps is the subject of many recent studies [1]. One of the simplest Hamiltonian maps exhibiting chaotic behavior is the standard, or Taylor–Chirikov [1, 2], map

$$\begin{aligned} I_{n+1} &= I_n + K \sin \theta_n, \\ \theta_{n+1} &= \theta_n + I_{n+1}, \end{aligned} \quad (1)$$

where  $I$ ,  $\theta$  are action–angle variables. It can be derived from the Hamiltonian of a one-dimensional periodically kicked rotor. More generally, it approximates several interesting nonlinear maps [2], and describes the local (in  $I$ ) behavior of a perturbed twist map [1, 2]. In this sense the map (1) is typical and representative. Its basic dynamical features were investigated in the pioneering work of Chirikov [2] and Greene [3]. In general, the map (1) displays all the three types of orbits: periodic cycles, KAM tori and chaotic orbits. The first two types of orbits (the regular ones) dominate

the  $(I, \theta)$  phase plane for small  $K$  ( $K \ll 1$ ) [2]. KAM tori extending over the entire  $\theta$  interval ( $0 \leq \theta < 2\pi$ ) divide the  $(I, \theta)$  phase plane into disconnected regions: orbits in one region cannot cross the bounding KAM tori into the other regions, so that the variations in  $I$  are bounded. However, it is now firmly established [1–4] that for  $K \geq K_c \approx 0.9716$  the bounding KAM tori break, making it possible for chaotic orbits to be unbounded in the  $I$  direction. At  $K_c$  the last, most “robust” KAM torus with the winding number  $w = 2\pi(\sqrt{5} - 1)/2$  [and the other equivalent KAM tori of (1) with winding numbers  $\pm w + 2\pi n$  ( $n$  integer)] disintegrates [3]. It corresponds to a non-analytic continuous curve, exhibiting fractal self-similar structure. The resulting scaling properties were established by renormalization group methods [5, 6]. The destruction of this last KAM torus signals the onset of global or connected stochasticity [3].

A major difficulty in the analysis of chaotic behavior of Hamiltonian systems is the proximity of chaotic and regular orbits on various scales [2]. Thus, for  $K \approx 1$ , the phase plane of (1) is an intricate mixture of regular and chaotic orbits [3].

†Address after September 1984, Department of Chemistry, University of Pennsylvania, Philadelphia, PA 19104, USA.

For  $K \gg 1$  chaotic orbits fill almost the entire phase plane, but “islets of stability”, in particular accelerator modes [2, 7], are known to exist for  $K$  arbitrarily large. When a chaotic orbit approaches such an islet, it may wander near it in a “regular” fashion. The area of each islet generally decreases when  $K$  increases.

Distinctive features of a stochastic or random motion, which allow a statistical description of it, are the rapid decay of correlations and diffusion. The decay of correlations in the chaotic region is related to the local instability, measured by the Lyapunov characteristic exponent [1, 2, 8]. For  $K \gg 1$ , the decay of correlations is actually exponential, with the decay exponent proportional to the Lyapunov exponent [8]. The existence of a definite characteristic time for the decay of correlations and the resulting statistical independence generally imply diffusion in the unbounded direction of the action  $I$  for  $K > K_c$  [see, e.g. ref. 1, sec. 5.4]. Therefore, a definite diffusion coefficient  $D$  can be associated with the chaotic motion

$$D = \lim_{n \rightarrow \infty} \frac{\langle (I_n - I_0)^2 \rangle}{n}, \quad (2)$$

where the average is taken over some large ensemble of initial positions  $(I_0, \theta_0)$  within the chaotic region. For large  $K$ , where the Lyapunov exponent is large, diffusion was verified unambiguously [2]. Moreover the diffusion coefficient  $D(K)$  approaches the asymptotic limit  $D_T = K^2/2$ . Improved approximate analytical expressions for  $D(K)$  were obtained using Fourier-space-path techniques [9–11]. The influence of an extrinsic random noise added to (1) on the diffusion coefficient  $D(K)$  was studied as well [7, 10, 11]. Since the map (1) is structurally unstable [2], random noise has the effect of destroying much of the interesting regular component (periodic cycles, KAM tori) existing for  $K \approx 1$ . Consequently  $D(K) \neq 0$  even for  $K < K_c$  [11]. Similarly, for  $K \gg 1$ , noise causes diffusion into, and out of, the islets of stability. In particular, it softens the effect of accelerator modes [7]. Note that for the accelerator

modes  $(I_n - I_0)^2 \approx n^2$  resulting in an infinite contribution to the diffusion coefficient. Consequently in the absence of noise  $D = \infty$  for values of  $K$  for which accelerator modes exist [2, 11].

For the map (1) (without any added noise) the diffusion coefficient vanishes for  $K \leq K_c$  but assumes a nonzero value for  $K > K_c$ . This transition is a result of the disappearance of the last bounding KAM torus and is somewhat reminiscent of thermodynamic phase transitions. Specifically, one would like to investigate the possibility of a singular power law behavior, namely

$$D(K) \propto (K - K_c)^\eta \quad (3)$$

for  $K \geq K_c$  in the vicinity of  $K_c$ , and to obtain  $\eta$  from some theory. It is reasonable to relate  $D(K)$  with the scaling of the disappearance of the last bounding KAM torus [5, 6]. Recently, MacKay, Meiss and Percival [12] have proposed a theory of transport in phase space for  $K > K_c$ . It assumes that the main obstacles to transport are the remnants of the KAM tori, called by them cantori. In this theory the motion is assumed to follow a random walk in the region between the cantori. It has some probability of reaching points in a strip about the cantorus, proportional to the width of that strip. The probability of crossing the cantorus is proportional to the phase-plane area escaping through it per iteration, if it is assumed to be uncorrelated with the way by which the strip was approached. In order to move a sufficiently large distance  $\Delta I$  (compared with  $2\pi$ ) one has to cross the cantorus. Therefore, this assumption implies that the probability of such an event, in a fixed number of time steps, is proportional to the escaping area. Consequently the diffusion coefficient is proportional to this quantity as well. For  $K \geq K_c$ , the escaping area is equal to the difference in action of cycles which approximate the cantorus [12, 13]. The scaling of this action is determined by the scaling of the disappearance of the last KAM trajectory [5, 6]. Thus, in this framework, the diffusion coefficient should satisfy the scaling form (3) with  $\eta \approx 3.01$ . Direct numerical calculations of

Chirikov [2], as well as the extrapolation to the limit of zero noise in the calculations of refs. 10, 11, 14, indicate that a relation of the form (3) is valid.

The present work is a detailed study of the mechanism of diffusion for the map (1) near  $K_c$ . In section 2 we present numerical evidence for the decay of correlations and diffusion in the interval  $1 < K \leq 2.5$ . In particular, we show that the system equilibrates in the stochastic layer on a time scale shorter than the one relevant for diffusion, namely  $t_d \approx 1/D$ . In section 3 we analyze the behavior of the diffusion coefficient  $D(K)$  in this interval of  $K$ . The numerical data are compared with the predicted critical behavior of the escaping area [12, 13], and the scaling (3) is verified in the entire interval. In section 4 we study the mechanism of diffusion of chaotic orbits through a cantorus. Evidence is given for the existence of a narrow stochastic channel connecting the chaotic region with the region of the cantorus. This channel lies near the subdominant symmetry line  $\theta = 0$  [5, 6], and mediates the transfer of chaotic orbits to the cantorus. This mechanism is different from the one naturally assumed [12] to relate the scaling of the diffusion coefficient with the disappearance of the last KAM torus. The route from the stochastic layer to the cantorus is found to exhibit fine structure rather than a simple random walk. A summary and conclusions are presented in section 5.

## 2. Decay of correlations and diffusion near $K_c$

A typical chaotic orbit for the map (1) at  $K = 1.1$  is shown in fig. 1. The orbit fills the “main stochastic separatrix layer” [1, 2], and does not enter into the central island about  $\theta = \pi$ , which is occupied by periodic cycles [1–3]. To have an idea of the decay of correlations and statistical dependence within the layer one may use the concept of the Lyapunov exponent, which, for the standard map, is equal to the KS-entropy [1, 2]. This can be

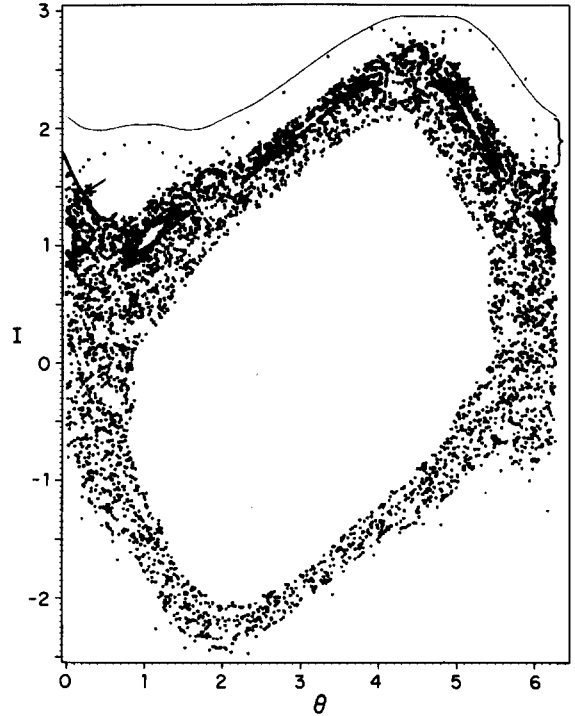


Fig. 1. A typical chaotic orbit for the standard map at  $K = 1.1$ . This orbit results from 5296 iterations starting from  $(I_0, \theta_0) = (0, 2\pi \cdot 948/1001)$ ; and terminating at the entrance of the channel (see section 4). Also displayed are the lower KAM torus, and the lower part of the channel, indicated by the arrow (compare with figs. 6 and 8). The bracket indicates the strip of periodic cycles separating the main stochastic layer from the cantorus (see section 4).

conveniently calculated as  $h \equiv \lim_{t \rightarrow \infty} h(t)$ , where

$$h(t) \equiv \frac{1}{t} \ln l_t = \frac{1}{t} \sum_{n=1}^t \ln \left( \frac{l_n}{l_{n-1}} \right). \quad (4)$$

Here  $l_n$  ( $n = 1, \dots, t$ ) are the lengths of vectors obtained by successively applying the tangent map of (1) on an initial unit vector  $l_0$ . The second equivalent expression for  $h(t)$  in (4) is useful for an accurate numerical calculation of  $h(t)$ , since it enables each of the  $l_n$ 's to be renormalized before an iteration in order to avoid divergences. In this way we have calculated (4) for several values of  $K$  near  $K \approx 1$  by using double-precision arithmetic (16 digits). For  $K > 1$  the asymptotic value of (4) appears to depend only slightly on the initial con-

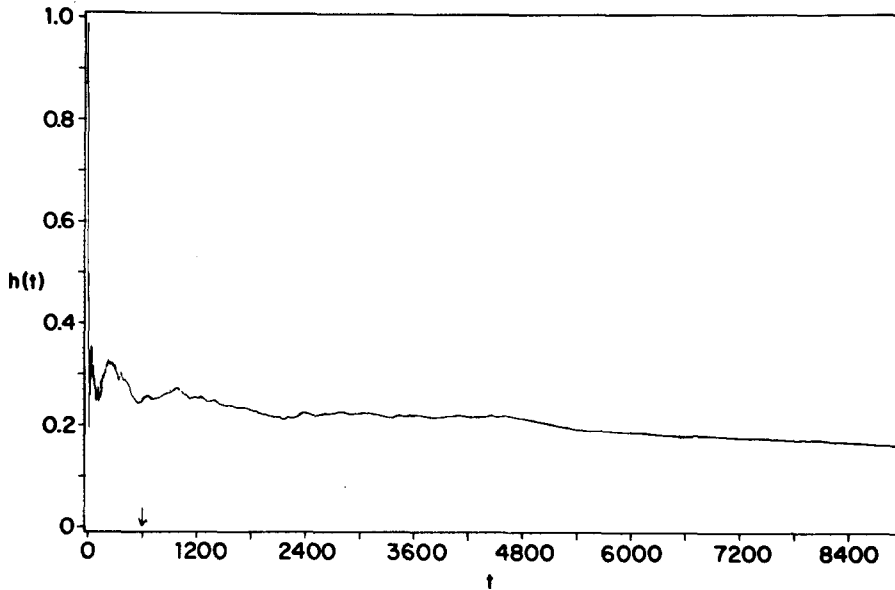


Fig. 2. The function  $h(t)$  of (4) for  $K = 1.1$ . The estimated relaxation time  $t_r$  is indicated by the arrow, while  $t_d \approx 3000$ .

ditions in the stochastic layer [2]. A typical behavior of  $h(t)$  for  $K = 1.1$  and  $t \leq 9000$  (which is of the order of the diffusion time, as considered later) is displayed in fig. 2. We see that  $h(t)$  varies wildly at small  $t$  but then relaxes to approximately its asymptotic value  $h \approx 0.16$ . The relaxation time  $t_r$  of  $h(t)$  gives an estimate of the time required for the chaotic orbit to explore the phase-plane area accessible to it between cantori (the equilibration time). The asymptotic value  $h$  of  $h(t)$  is the Lyapunov exponent which is related [2, 8] to the typical time  $t_c \approx 1/h$  of the decay of correlations. Thus, for  $K = 1.1$ , the memory of initial-state correlations is completely lost after a time of the order of 10 iterations. In double-precision arithmetic, used throughout this work, roundoff errors accumulate to a 100 percent uncertainty in the position of the chaotic orbit after approximately  $n_{\max} = 16 \ln 10/h \approx 230$  iterations. Consequently, the trajectory calculated by iterating (1) thousands of times, such as that shown in fig. 1, does not represent a true chaotic orbit. However, it may correspond to an ensemble of short pieces of true chaotic orbits starting from different initial conditions in the stochastic layer. Thus, quantities asso-

ciated with large ensembles of trajectories (such as the diffusion coefficient (2)) should not be affected significantly by roundoff errors.

The fast decay of correlations indicates that the motion in the region between cantori rapidly reaches statistical independence. We are interested in testing whether this fact implies that on longer time scales, required to cross the cantori, the motion is diffusive. It is instructive to introduce the diffusion time  $t_d \approx 1/D$  so that on time scales larger than  $t_d$  the motion can be considered diffusive. Generally we have found that  $t_d \gg t_r$ . This means that the motion equilibrates in the region between cantori, namely it reaches its equilibrium KS-entropy in this region, on a time scale much shorter than the diffusion time, or much before transport through a cantorus takes place (see also section 4). For times  $t$ ,  $t_r < t < t_d$  the motion looks bounded and chaotic. The correlations decay even faster since  $t_c \ll t_r$ . The separation among the various time scales verifies one of the assumptions of the theory suggested by MacKay et al. [12]. It was verified that diffusion indeed takes place by choosing a proper unit of time containing  $t_d$  iterations and plotting  $\langle (I_{m t_d} - I_0)^2 \rangle$ , for  $m = 1, \dots, 50$ ,

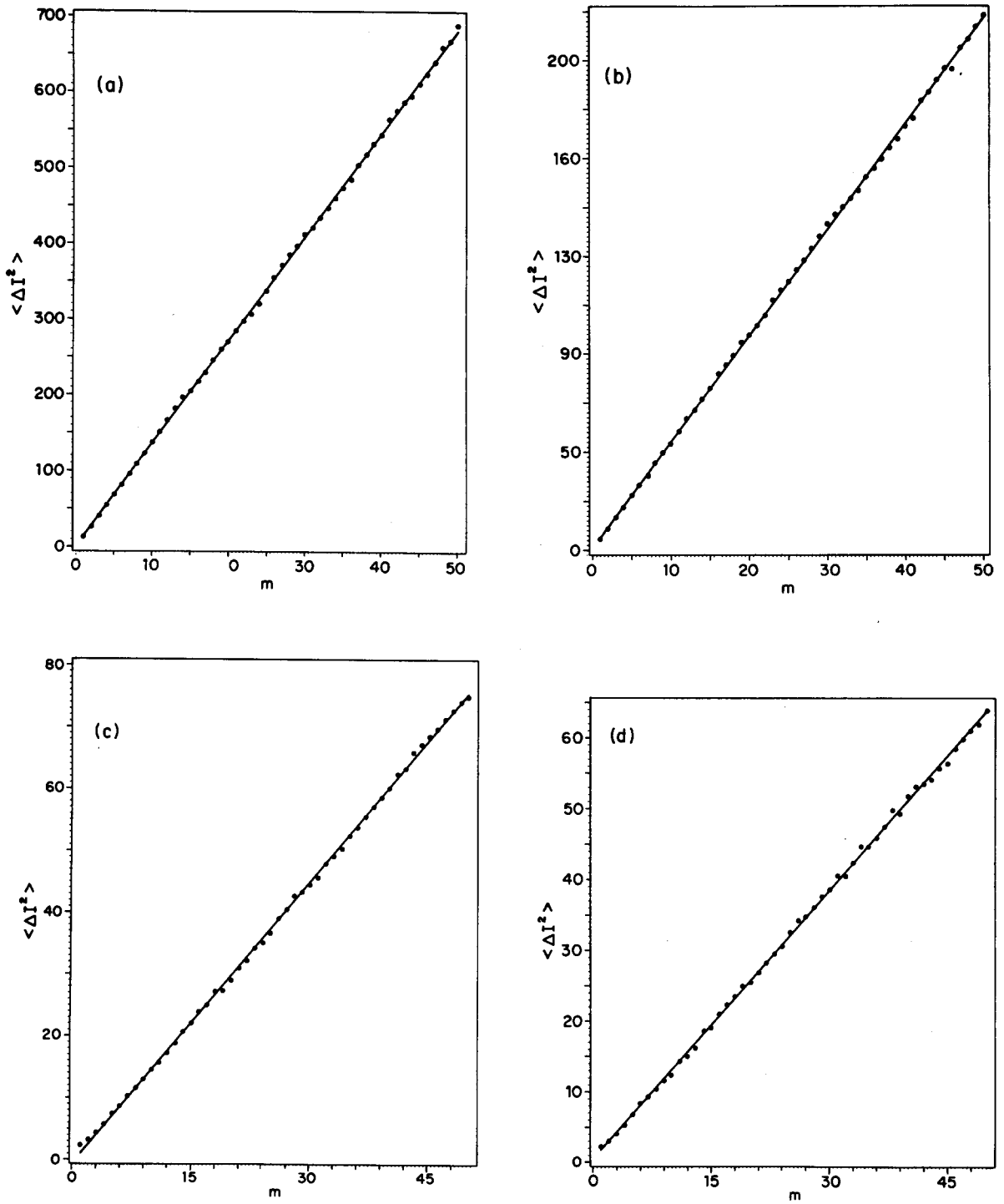


Fig. 3. Plots of  $\langle \Delta I^2 \rangle \equiv \langle (I_{m,t_d} - I_c)^2 \rangle$  versus  $m$  ( $m = 1, \dots, 50$ ) for (a)  $K = 2.3$ ; (b)  $K = 1.575$ ; (c)  $K = 1.212$ ; (d)  $K = 1.092$ . Also plotted are the straight lines corresponding to the least-squares fits of the numerical data.

versus  $m$ . The average  $\langle \rangle$  was taken over an ensemble of initial positions  $(I_0, \theta_0)$ , where  $I_0 = 0.01$  and  $\theta_0$  assumes 5000 values uniformly spread in the interval  $(0, 2\pi)$ . We have eliminated of course trajectories starting in the central island around  $\theta = \pi$  which do not contribute to diffusion. Some examples of these plots are given in fig. 3, which indeed show a nice diffusionlike behavior. The diffusion coefficient (2) was calculated as the slope (divided by  $t_d$ ) of the straight line which is the least-squares fit of the numerical data (shown in fig. 3 as well). We have assumed that the deviations of the data points from the straight line result from statistical uncertainties. This uncertainty was estimated as twice the mean-square-root deviation of the data points from the straight line. The statistical uncertainty  $\Delta D$  in  $D$  was calculated accordingly. For all the values of  $K$  considered in the interval  $(1, 2.5)$  the relative uncertainty  $\Delta D/D$  was always less than 2% and in many cases less than 1%. We have also compared the values of  $D$  obtained by performing the statistical average in (2) over different subsets of the original ensemble  $\{(I_0, \theta_0)\}$ . Here the statistical deviations  $\Delta D/D$  did not exceed 3%. Accurate results were generally obtained when the time unit  $t_d$  was chosen consistently with the mean diffusion time,  $t_d \approx 1/D$ .

Measuring diffusion near  $K_c$  requires iterating the map (1) many times because of the large diffusion time  $t_d$ . The accuracy of the results requires taking the average in (2) over a reasonably large ensemble of initial positions. For example, for  $K = 1.125$ , with  $t_d = 2500$  and with an ensemble of 5000 initial positions, we obtained the value  $D = 5.46 \times 10^{-4}$  with an accuracy of 0.88%. This required approximately 1.5 hours cpu time on an IBM 3081 computer. Such long computer times forced us to restrict our calculations to the interval  $1 < K \leq 2.5$ .

### 3. Evidence for the scaling behavior of the diffusion coefficient

We have calculated numerically the diffusion coefficient  $D(K)$  at various values of  $K$ . In order

to test the scaling law (3) we have plotted in fig. 4  $\ln D(K)$  versus  $\ln \Delta K$ , where  $\Delta K \equiv K - K_c$ . We have found that the calculated data points are concentrated around some straight line. A least-squares fit of all data points in the interval  $1 < K \leq 2.5$  (fig. 4a) yields a slope  $\eta_0 \approx 3.24$ . If one takes into account only data in the vicinity of the critical point,  $1 < K < 1.4$ , displayed in fig. 4b, one finds a slope  $\eta_1 \approx 3.16$ . The data in the interval  $1.4 \leq K \leq 2.5$  (plotted in fig. 4c) gives a slope  $\eta_2 \approx 2.96$ . These values of  $\eta_0$ ,  $\eta_1$  and  $\eta_2$  should be compared with the asymptotic value  $\eta \approx 3.01$ , predicted by the scaling theory of the disappearance of the last bounding KAM torus [12, 13]. Within the accuracy of our data we can observe oscillations around the straight lines in fig. 4. In order to understand these oscillations, let us recall the scaling relation satisfied by the flux of phase-plane area escaping through a cantorus per iteration [12]:

$$\Delta W = A(\Delta K)^\eta U_1(\log_\delta \Delta K) + B(\Delta K)^{\eta'} U_2(\log_\delta \Delta K) + \dots, \quad (5)$$

where  $A$  and  $B$  are constants  $\eta \approx 3.01$ ,  $\eta' \approx 4.02$  and  $\delta \approx 1.63$ . The functions  $U_1(x)$  and  $U_2(x)$  are periodic functions of  $x$  that satisfy  $U_1(x+1) = U_1(x)$  and  $U_2(x+1) = -U_2(x)$ . The function  $U_1(x)$  has a large constant component [6, 12]. Thus, the first leading term on the r.h.s. of (5) has a small superimposed periodicity in  $\ln(\Delta K)$  with period  $\Delta \ln(\Delta K) = \ln \delta \approx 0.487$ . The second term is an intrinsic correction with a periodicity in  $\ln(\Delta K)$  of twice this period. Such a correction should be taken into account already for  $\Delta K = 0.1$ , where the value of  $\Delta W$  calculated numerically differs by 10% from the value calculated from the leading term in (5) [12]. We have verified that the period of the oscillations of  $\ln D(K)$  is indeed of the magnitude of  $\ln \delta$ , but more precise statements cannot be made on the basis of our data.

We would like to mention that oscillations in  $D(K)$  near the critical region may already be seen in the data of Chirikov [2]. A critical behavior in

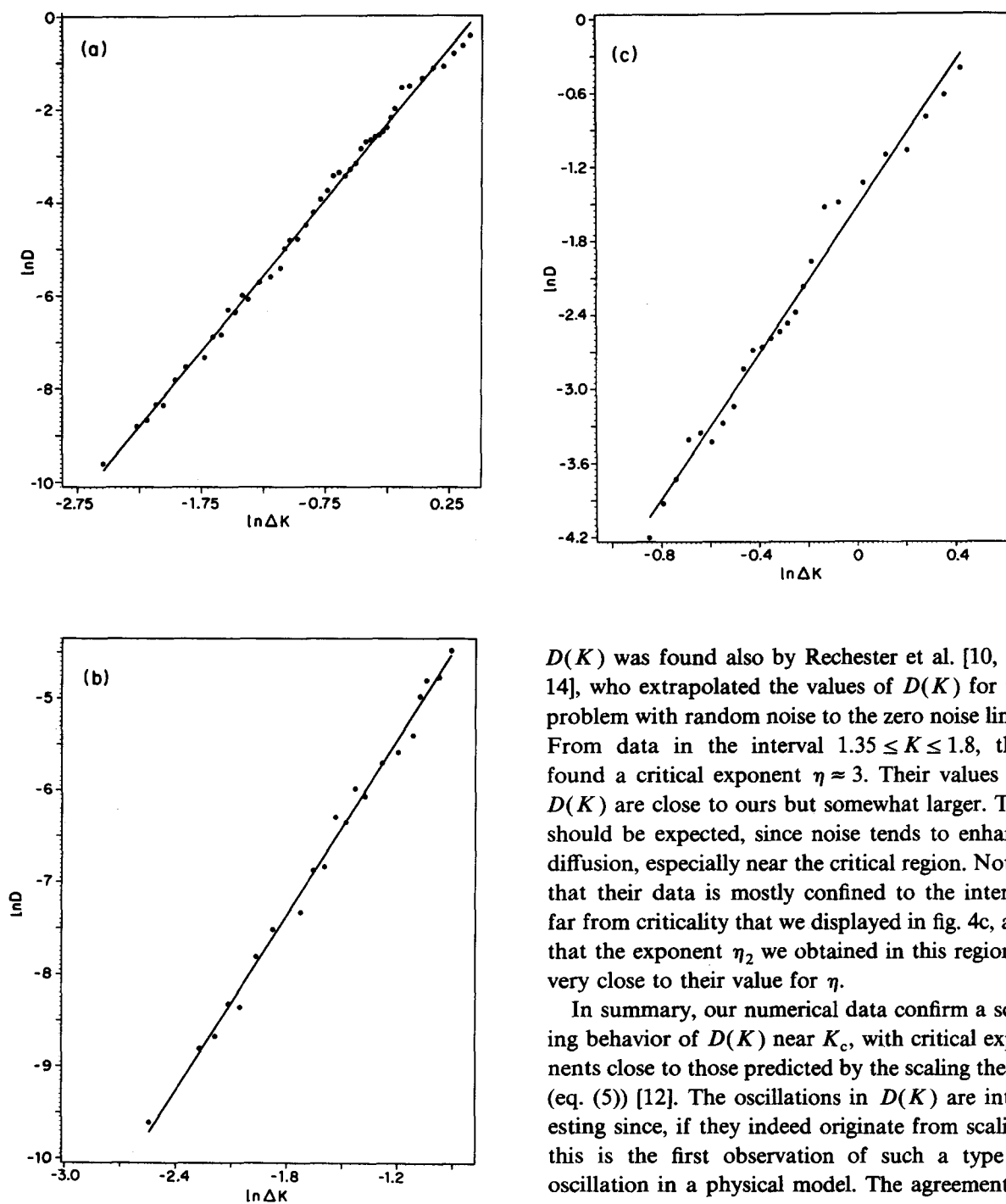


Fig. 4. Plots of  $\ln D(K)$  versus  $\ln \Delta K$  in several intervals of  $K$ : (a)  $1 < K \leq 2.5$ ; (b)  $1 < K < 1.4$ ; (c)  $1.4 \leq K \leq 2.5$ . The straight lines correspond to the least-squares fits of the numerical data in each interval.

$D(K)$  was found also by Rechester et al. [10, 11, 14], who extrapolated the values of  $D(K)$  for the problem with random noise to the zero noise limit. From data in the interval  $1.35 \leq K \leq 1.8$ , they found a critical exponent  $\eta \approx 3$ . Their values for  $D(K)$  are close to ours but somewhat larger. This should be expected, since noise tends to enhance diffusion, especially near the critical region. Notice that their data is mostly confined to the interval far from criticality that we displayed in fig. 4c, and that the exponent  $\eta_2$  we obtained in this region is very close to their value for  $\eta$ .

In summary, our numerical data confirm a scaling behavior of  $D(K)$  near  $K_c$ , with critical exponents close to those predicted by the scaling theory (eq. (5)) [12]. The oscillations in  $D(K)$  are interesting since, if they indeed originate from scaling, this is the first observation of such a type of oscillation in a physical model. The agreement of the critical behavior of  $D(K)$  with the predictions of scaling theory calls for a more detailed study of the mechanism of diffusion, which will be the subject of the next section.

#### 4. A mechanism of transport through a cantorus

The map (1) is essentially periodic in both variables  $I$  and  $\theta$  with the period  $2\pi$ . In the basic zone  $0 \leq I < 2\pi$ ,  $0 \leq \theta < 2\pi$ , and for  $K \leq K_c$ , there are two equivalent (under inversion  $(I, \theta) \rightarrow (-I, -\theta)$  and translation by  $2\pi$ ) KAM tori, having winding number  $w_+ = 2\pi(\sqrt{5} - 1)/2$  and  $w_- = 2\pi(3 - \sqrt{5})/2$ . These tori divide this basic zone into two disconnected regions (see fig. 5): a “small” region between the tori (denoted  $R_s$ ), and a “large” region outside them. The latter region consists of two parts,  $R_u$  and  $R_d$ , which are actually connected with the regions  $R_d$  and  $R_u$ , respectively, in the neighboring zones. Periodic, quasiperiodic and chaotic orbits exist in both regions, and for  $K \leq K_c$ , they are localized within these regions. For  $K > K_c$ , the bounding KAM tori break, and chaotic orbits can move in the  $I$  direction from one region to the other [3].

In what follows we shall study in some detail the mechanism of diffusion of chaotic orbits starting within the “large” region ( $R_d$ , for example). These orbits form the “main stochastic layer” [2] (see figs. 1 and 5) which is separated from the KAM

tori for  $K \leq K_c$  (or from their remnants, i.e. the cantori [12], for  $K > K_c$ ) by narrow strips, where periodic cycles, approximants of the KAM tori [3], lie. Such a strip is indicated by a bracket in fig. 1. Chaotic orbits diffusing out of the stochastic layer must wander in these strips before crossing the cantori. We study how the transport from the layer to the cantori takes place within these strips.

A main difficulty one faces in answering such a question is caused by the roundoff errors which prevent one from following a chaotic orbit for many iterations reliably. Therefore an ensemble of trajectories will be studied according to the following procedure. Consider the strip separating the stochastic layer from the lower KAM torus having winding number  $w_- = 2\pi(3 - \sqrt{5})/2$  (the motion in the other strip is equivalent to the one in this strip by inversion symmetry, and will not be considered therefore any further). Within this strip we trace an imaginary line  $L_i$  which is parallel to the KAM torus and lies a distance  $\Delta I_i$  below it (for example, any of the lines a, b, c, d in fig. 6). We take  $\Delta I_i \leq J$ , where  $J$  is the approximate width of the strip, where the periodic approximants of the KAM tori lie. The stochastic layer is outside of

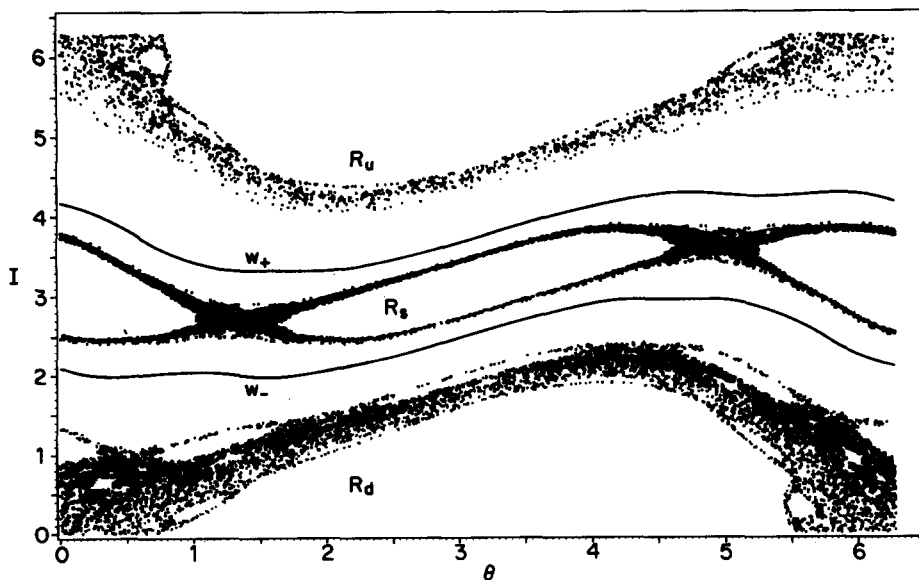


Fig. 5. Four orbits of the standard map at  $K = K_c \approx 0.9716$  in the basic zone  $0 \leq I < 2\pi$ ,  $0 \leq \theta < 2\pi$ .



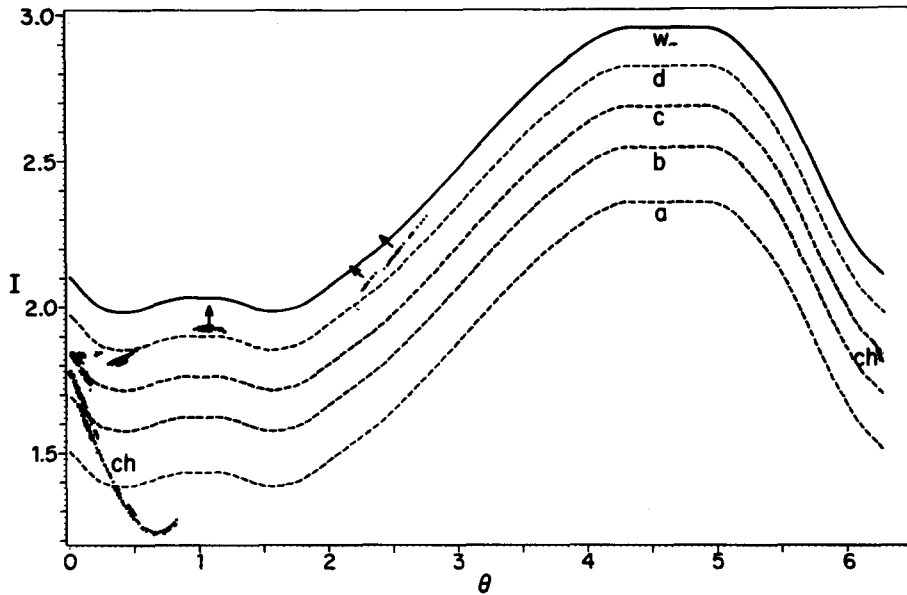


Fig. 6. The stochastic channel (ch) mediating transport for  $K = 1.1$ , constructed as described in section 4. Also displayed are the lower KAM torus ( $w_-$ ), and some of the imaginary lines (a, b, c, d) used for constructing the channel. The final sets of points which cross the KAM torus in the following iteration are indicated by the arrows.

this strip. For each line  $L_i$  one finds the set  $S(\Delta I_i)$  of points  $(I_s, \theta_s)$  having the following properties: (a) each point  $(I_s, \theta_s)$  belongs to a chaotic orbit starting from some initial condition within the stochastic layer; (b)  $(I_s, \theta_s)$  lies below  $L_i$ ; (c) repeated applications of the map ultimately transform  $(I_s, \theta_s)$  into some point  $(I_t, \theta_t)$  above the KAM torus; and, finally, (d) *all* subsequent iterations of  $(I_s, \theta_s)$ , before  $(I_t, \theta_t)$  is reached, lie above  $L_i$ . If the approach to the KAM torus within the strip were homogeneous, the set of points  $S(\Delta I_i)$ , for all  $\Delta I_i \leq J$ , would be spread homogeneously below  $L_i$ . For  $K \leq K_c$  the sets  $S(\Delta I_i)$  are obviously empty.

This analysis was performed at  $K = 1.1$ . It is assumed that for this value of  $K$  the shape of the cantori is only slightly distorted relative to that of the KAM tori at  $K = K_c$ , so that the cantorus can be replaced by the corresponding KAM torus. This assumption is justified a posteriori later. The width of the strip was estimated as  $J \approx 0.6$ . Taking a statistic of approximately 300 initial conditions within the stochastic layer on the line  $I = 0$ , and

iterating the map 6000 times (which is of the order of the diffusion time), we have plotted the sets  $S(\Delta I_i)$  for a sequence of lines  $L_i$ . The interval in  $\Delta I_i$  between neighboring lines was chosen between 0.04 and 0.02. The results are summarized in fig. 6, where some of the lines  $L_i$  are displayed as well. It is quite evident from fig. 6 that the sets  $S(\Delta I_i)$  are strongly localized in the phase plane and form a kind of "stochastic channel", which approaches the cantorus near the "subdominant" symmetry line  $\theta = 0$ . It is easily seen that this channel mediates the transfer to the cantorus in the following way. A chaotic orbit can advance effectively in the  $I$  direction only after it "finds" the channel. From here it can enter into a strip between two imaginary lines and move parallel to them until it "finds" a "higher" part of the channel in this strip, and so on. We have checked that orbits entering the strips between the lines not through the channel are reflected back just after very few iterations and cross many times the lines from both sides until the channel is "found". In some cases these orbits return to the stochastic layer. We

followed them during the entire simulation time as well. In general, the chaotic orbits spend a large fraction of their diffusion time in the stochastic layer, but when the channel is found the effective transport in the  $I$  direction takes place rapidly. Thus, for example, the trajectory in Fig. 1 finds the channel only after 5296 iterations, but then just 110 iterations are sufficient to reach a point  $(I_f, \theta_f)$  above the cantorus. On the other hand, the trajectory in fig. 7 finds the channel just after 567 iterations, and then only 28 iterations are sufficient to reach  $(I_f, \theta_f)$ . We have verified that all the trajectories that crossed the cantorus during the simulation approached it via the channel. The channel is therefore the route that a trajectory, starting in the stochastic layer, has to take in order to cross the cantorus. The existence of the channel and the mechanism of diffusion described above have been verified also for other values of  $K$  in the vicinity of  $K_c$ .

The final sets of points which will cross the cantorus in the following iteration are indicated by arrows in fig. 6. It should be pointed out that these sets of points do not reflect the only gaps of the cantorus. In fact, we have checked that at subsequent iterations the chaotic orbits cross the cantorus from both sides at different gaps, until they are transferred effectively in the region  $R_s$  above the cantorus (see fig. 5). We have applied this procedure for constructing the channel above the cantorus but with an imaginary line parallel to it and lying a distance  $\Delta I = 0.2$  above it playing the role of the cantorus in the definition of the set  $\Delta S(w_-)$  (from fig. 5 we see that this line touches the second order stochastic separatrix layer in the region  $R_s$ ). The resulting channel is displayed in fig. 8, and, as one could expect, it differs from the channel in fig. 6 only in the "higher" part, that lies near  $w_-$ . In any case, the channel is localized near the subdominant symmetry line  $\theta = 0$ .

These results indicate that the approach to the cantorus takes place quite inhomogeneously, at least from the main stochastic layer. The existence of a strongly localized channel mediating transport, and the related motion parallel to the imag-

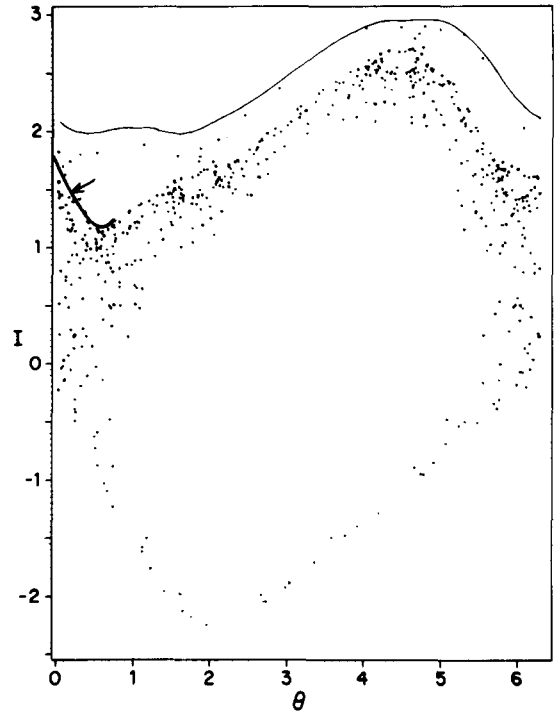


Fig. 7. Same as fig. 1, but for an orbit which finds the channel after 567 iterations starting from  $(I_0, \theta_0) = (0, 2\pi \cdot 927/1001)$ .

inary lines, also indicate that these lines, which were chosen arbitrarily, reflect actually a true structure. Comparison with the structure for  $K = K_c$  indicates that the lines should nearly follow the periodic cycles approximating the cantorus [1, 6, 12]. This justifies a posteriori the replacement of the cantorus by the KAM torus at  $K_c$ .

It is known [2] that diffusion near  $K_c$  is mainly due to a random transition between adjacent stochastic layers, with the diffusion time at least of the order of a typical transition time. In fact, comparison of figs. 1 or 7 with fig. 6 suggests that the lower part of the channel (which approaches monotonously the subdominant symmetry line  $\theta = 0$ ) may result from the overlap of the third order stochastic layer (surrounding the periodic cycle of winding number  $1/3$ ) with the fourth order stochastic layer which is engulfed by the main layer. The part of the channel which is closer to the cantorus (see figs. 6 and 8) may result similarly from the overlap of higher order stochastic layers.

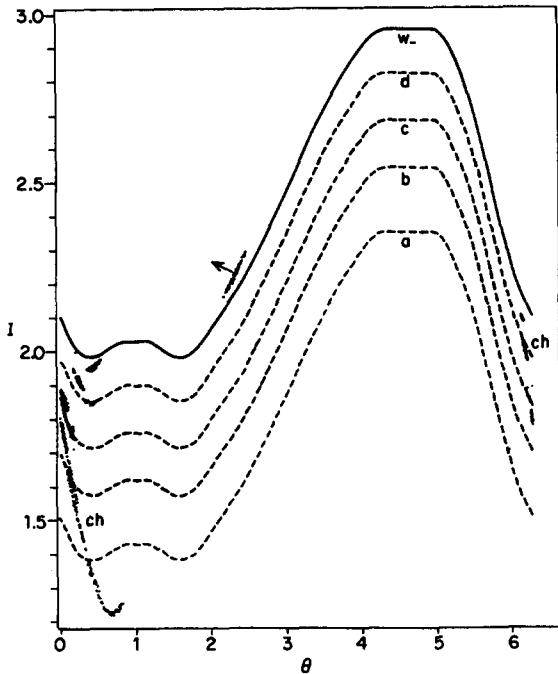


Fig. 8. Same as fig. 6, but with the final set of points (indicated by the arrow) crossing in the following iteration an imaginary line parallel to the KAM torus and lying a distance  $\Delta I = 0.2$  above it.

Despite the fact that the layers overlap in several parts of the interval  $0 \leq \theta < 2\pi$ , the channel is localized in a definite region, namely near the subdominant symmetry line  $\theta = 0$ . This is plausible, since on this line two-thirds of the cycles are hyperbolic [5, 6], and trajectories starting in the chaotic region cannot approach elliptic cycles. Thus, the subdominant symmetry line seems to be a most favorable direction for transport near  $K_c$ .

In the previous section we have verified that the scaling behavior of the diffusion coefficient  $D(K)$  near  $K_c$ , is quite close to that obeyed by the flux of phase-plane area escaping through a cantorus per iteration [12, 13] (see eqs. (3) and (5) and fig. 4). It is remarkable that, in spite of the fine structure of the route to the cantorus, which includes a narrow channel, such an agreement between the critical behavior of  $D(K)$  and the simple scaling law (3) holds. Critical narrowing of the channel may result in an exponent  $\eta$  larger than the one in eq. (5).

Because of numerical difficulties we could not investigate the behavior of  $D(K)$  and the possibility of such a narrowing in the close vicinity of  $K_c$  ( $K_c < K < 1$ ). In this work an ensemble of trajectories was studied. Thus, the long time correlations among phase-plane points of definite trajectories, before and after crossing the cantorus, were not considered. These correlations may be important for the relation between diffusion and the flux of phase-plane area escaping through a cantorus.

## 5. Summary and conclusions

The properties of transport in the phase-plane were studied for the standard map. We have verified that for  $K$  near  $K_c$ ,  $K > K_c$ , the motion is diffusive on a sufficiently long time scale. In the vicinity of  $K_c$  the main obstacles to diffusion are the remnants of the last KAM bounding torus (or cantorus). In the regions between cantori the chaotic motion equilibrates fast, in the sense that the KS-entropy relaxes in a time much shorter than the characteristic diffusion time. We have found that to a good approximation the diffusion coefficient follows the scaling in  $\Delta K = K - K_c$  of the phase-plane area escaping through a cantorus [12, 13]. This scaling was verified on a surprisingly large interval of  $K$ , namely  $1 < K \leq 2.5$ .

We have established the existence of a narrow channel mediating transport from the main stochastic layer to the neighborhood of a cantorus. This channel crosses the strip where the periodic cycles approximating the cantorus lie, and approaches the cantorus near the subdominant symmetry line  $\theta = 0$ . Consequently the trajectories escaping through the cantorus follow a path exhibiting quite a delicate structure in the strip. Such a structure was not considered in earlier studies [12] but a simple random walk between cantori was assumed. One might expect that this structure would lead to deviations from the proportionality between the diffusion coefficient and the phase-plane area escaping through the cantorus. In our

numerical studies such deviations were found to be small. Because of numerical difficulties (long computer time required) we could not study the immediate vicinity of the critical point ( $K_c < K < 1$ ). Therefore the relative importance of the deviations from (5) in this region is not known. This point is left to further studies. It is quite possible that the predictions of the scaling theory hold in spite of the existence of the specific route to the cantorus studied in the present work. It may reflect the scaling satisfied by the approximants of the KAM torus in its surrounding strip [6].

### Acknowledgements

This work was supported in part by the U.S.-Israel Binational Science Foundation (B.S.F.), and by the Bat-Sheva de Rothschild Fund for Advancement of Science and Technology. We thank P. Bak, D. Bensimon, M.V. Berry, S.N. Coppersmith, M. Feingold, L.P. Kadanoff, I.C. Percival, I. Procaccia and A.B. Rechester for useful discussions and correspondence. S.F. thanks R.E. Prange for critical reading of the manuscript and for the hospitality of the University of Maryland where work was completed with support from the NSF through grant No. DMR-79-001172-A02.

### Note added in proof

The actual value of the diffusion coefficient  $D$  (calculated in Section 2) depends on the initial

conditions, since a fraction of the trajectories start in islets of stability and are trapped there (we thank B.V. Chirikov for drawing our attention to this point). However, the critical properties of  $D$ , that are the subject of this work, do not depend on initial conditions if these are outside the strip where the cycles that approximate the critical KAM trajectory lie. In this work such initial conditions were used.

### References

- [1] A.J. Lichtenberg and M.A. Lieberman, *Regular and Stochastic Motion* (Springer, Berlin, 1983); and references therein.
- [2] B.V. Chirikov, *Phys. Rep.* 52 (1979) 263; and references therein.
- [3] J.M. Greene, *J. Math. Phys.* 20 (1979) 1183.
- [4] J.N. Mather, *Topology* 21 (1982) 457.
- [5] L.P. Kadanoff, *Phys. Rev. Lett.* 47 (1981) 1641; S.J. Shenker and L.P. Kadanoff, *J. Stat. Phys.* 27 (1982) 631; L.P. Kadanoff, in: *Melting Localization and Chaos*, R.K. Kulik and P. Vashista, eds. (North-Holland, New York, 1982).
- [6] R.S. MacKay, *Renormalization in Area-Preserving Maps*, Ph.D. Thesis, Princeton (1982).
- [7] C.F.F. Karney, A.B. Rechester and R.B. White, *Physica* 4D (1982) 425.
- [8] C. Grebogi and A.N. Kaufman, *Phys. Rev.* A24 (1981) 2829.
- [9] H.D.I. Abarbanel, *Physica* 4D (1981) 89.
- [10] A.B. Rechester and R.B. White, *Phys. Rev. Lett.* 44 (1980) 1586.
- [11] A.B. Rechester, M.N. Rosenbluth and R.B. White, *Phys. Rev.* A23 (1981) 2664.
- [12] R.S. MacKay, J.D. Meiss and I.C. Percival, *Phys. Rev. Lett.* 52 (1984) 697; *Physica* 13D (1984) 55.
- [13] D. Bensimon and L.P. Kadanoff, *Physica* 13D (1984) 82.
- [14] A.B. Rechester, private communication.